SHAKING TABLE TEST AND ANALYSIS ON ULTIMATE CHARACTERISTICS OF LEAD RUBBER BEARING FOR BASE ISOLATED FBR PLANT

Nobuhisa SATO[1], Yukio WATANABE[2], Asaro KATO[2], Masaaki OHBA[2],
Yasuaki FUKUSHIMA[1], Masao IIZUKA[1], Kazuhide YOSHIKAWA[1], Katsuhiko UMEKI[3]
Junji SUHARA[4], Yasuyuki Murazumi[5],Genji Yoneda[6]

SUMMARY

INTRODUCTION

A DFBR plant in Japan is to be planned as a base isolated building in the horizontal direction. LRB is considered as one of the base-isolation systems. The seismic margin and the ultimate behavior of LRB were verified through the shaking table tests using the reduced scaled model of a DFBR with LRBs and the simulation analyses using the polygonal lines as well as in the case of NRB as the authors reported in 12th SMiRT[1].

THE SHAKING TABLE TESTS

Test Methods

Input Condition

The test cases are shown in table.1. Four excitation levels were set up in these tests. Those were on the design level, the hardening level, the level established as the design limit, and the target breaking level of the LRB. The time scale were reduced by one-fourth using the Similarity Law where the reduced scale of acceleration and stress of the base-isolation system was the same as full scale.

Test Model

The test model was 2500(wide)･2000(deep) ･3500mm(high), and is about one-sixteenth the scale of the base isolated DFBR building model. The model consisted of a superstructure and a base-isolation system. The outline of the model is shown in Fig.1.

(a) The superstructure

The superstructure had three floors and was made of steel. Its total weight was about 17 tonf. The second floor of the superstructure was modeled as the reactor support floor of a DFBR. The first-story column was made of high strength steel so as to remain elastic through out the experiment.

(b) The base-isolation system

The vertical stress of the LRB was 50 kgf/cm^2. The period corresponding to the initial stiffness of the base-isolation system was equal to 1.0 second for the full scale building. The period corresponding to the second stiffness was equal to 2.0 seconds. The ratio of yield shear stress to design vertical stress of the LRB was 0.05. These figures are used in the standard design of DFBR's in Japan. The total thickness of the rubber sheet of the

[1]*Kajima Corporation, Tokyo, JAPAN Fax:+81-3-5561-2345*
[2]*The Japan Atomic Power Company, Tokyo, JAPAN Fax:+81-3-3212-8463*
[3]*Obayashi Corporation, Tokyo, JAPAN Fax:+81-3-5247-8681*
[4]*Shimz Corporation, Tokyo, JAPAN Fax:+81-3-5441-0370*
[5]*Taisei Corporation, KANAGAWA, JAPAN Fax:+81-45-224-2345*
[6]Takenaka Corporation, Tokyo, JAPAN Fax:+81-3-3545-0974

LRB was 7mm. The shape of the LRB is shown in Fig.2. Four LRBs were placed under the superstructure columns in the test.

The Shaking Table

The six degree-of-freedom shaking table was used.

Measurements

Horizontal accelerations were measured at each floor and at the top of the shaking table. Horizontal relative displacement and shear force of the isolated layer were also measured. As a result of these tests measurements, dynamic characteristics of the superstructure and the base-isolation system can be evaluated. Vertical relative displacement and vertical force of the LRB were measured in particular for analyzing the failure mode of the LRB. Moreover, instruments were chosen for their durability throughout the tests: they had to be strong enough to handle the vibration when the LRB broke.

Static Tests Of Lrb

Three types of static tests for the LRBs were conducted. Those were: 1. The static tests for every specimen in a factory prior to the shaking table tests, 2. Static breaking tests by a monotonic load under the design vertical stress and 3. Static failure limit tests.

・The quality of the LRBs were confirmed from the results of the static tests for every specimen in a factory prior to the shaking table test. The outline of the static tests are as follows:

parameter : shear strain = 100,150,200%
: the vertical stress= 50kgf/cm^2 (design value)
loading : 4 times cyclic loading under a design vertical load.
Measurements : Mean shear modulus and mean force at 0 displacement for the third cycle are shear stiffness (K_H) and characteristic dissipator shear strength (Qd) of the LRBs respectively.

The results are shown in Fig.3. The static test results were approximately within ±10% of the design value.

・Static breaking tests by a monotonic load under a design vertical stress were also conducted. Using the results of the tests, the shear strain linear limit of the LRB could be calculated[3]. When the linear limits were calculated, the characteristic dissipator shear strength was used for the results of the former tests (shear strain 200%).

The calculated shear strain linear limit was approximately 310%. The test results were also compared with the shaking table tests. The average of the breaking strain was approximately 530%.

・Static failure limit tests utilizing two directional loads for calculating the breakage bound were conducted. The outline of the static tests are as follows:

number : five test pieces for the LRBs
test cases : i. shear breaking test in the compressive zone (vertical stress :250kg/cm^2)
ii. shear breaking test under non vertical loading
iii. shear breaking test in the tensile zone (vertical strain : 25%)
iv. shear breaking test in the tensile zone (vertical strain : 50%)
v. tensile breaking test
method : static monotonic loading[1]

As a result of static break tests utilizing a monotonic load under a design vertical stress and static failure tests using two directional loads, the static breakage bound of the LRB was confirmed. Additionally, the breakage bound is compared with the shaking table tests. Test results and the breakage bound will be shown later.

Test Results

Input Motion Of The Shaking Table

The acceleration response spectra of the shaking table at each input point are shown in Fig.4. In this figure the response spectra for $5 \times S_2$ input was calculated using the data until the rubber broke. This figure showed that the ratio of the response spectra at amplified S_2 input to $1 \times S_2$ input was almost directly proportional to coefficient of amplified S_2 input in the period of 0.25 to 0.5 second; the initial natural period of the LRB to the second natural period of the LRB.

Shear Force – Horizontal Displacement Hysteresis Curve Of Isolated Layer

The LRB hysteresis curves of shear force - horizontal displacement at $1 \times S_2$, $2 \times S_2$, and $5 \times S_2$ input are shown in Fig.5. In Fig.5(d) the hysteresis in the third quadrant were rotated by 180 degrees. This figure also shows the breaking point of the LRB and the results which were four times as much as the stress of the static breaking tests under a monotonic load. The maximum horizontal shear strain of the isolator at $1 \times S_2$ input was about 80%. This strain was under the linear limit. The maximum horizontal shear strain of the isolated layer at $2 \times S_2$ input was about 310% which was almost the linear limit. The maximum horizontal shear strain of the isolated layer at $3 \times S_2$ input was about 490%, but not all the LRBs broke. One of the LRBs (A3 in Fig.1) broke near the maximum strain which was about 640% at $5 \times S_2$ input. Immediately after that, the rest of the LRBs broke on the opposite side. When the hysteresis was compared with the static breaking tests, the slip phenomena could be seen from the hysteresis at $4 \times S_2$ input clearly, the breaking strain of the shaking table test was greater than the static breaking tests.

Failure Mode For The Rubber Bearings

The failure mode for the LRBs is shown in Fig.6. In the vertical strain - horizontal shear strain relation and the vertical stress - horizontal shear strain relation, the breakage bound which was calculated by the static breaking tests was included. The vertical stress at the breakage of the LRB which broke first among the four elements was at about 30 kgf/cm^2 on the tension side, the vertical strain was about 10 % for the LRBs as is shown in Fig.6. That is to say, the LRB broke in the tension-shear zone. The breaking strain of all the LRBs which broke during the shaking table tests was greater than that of the static breaking tests and the strain was also beyond the breakage bound.

THE SIMULATION ANALYSES OF THE SHAKING TABLE TESTS

Analytical Conditions

Input Conditions

The input waves for the analyses were acceleration waves, which were observed on the shaking table during the shaking table tests. The acceleration response spectra for each input are shown in Fig.4.

Simulation Model

(a) The superstructure
The superstructure of the reduced-scaled base isolated DFBR was modeled as lumped masses, shear springs and rotation springs. The values of the springs were set up by the transfer function of the sweep tests before conducting the shaking table tests. The simulation analysis model is shown in Fig.7.
(b) The base-isolation system
The base-isolation system was modeled as two shear springs in the horizontal direction, because the system consists of the RB and the lead plug. One of the shear springs was modeled as a RB and the another modeled as a lead plug. The RB was modeled using polygonal lines, taking into account a slip phenomenon. The slip phenomenon considers that the horizontal displacement at the beginning stage of the hardening increases due to the influence exerted by cyclic loading. The input level for each excitation was greater than the previous excitation and the LRBs were not replaced at each excitation. That condition was also considered for the simulation analyses. A lead plug was modeled as an elasto-plastic model. The base-isolation system was modeled as an axial spring in the vertical direction. The spring was elastic within the compressive zone and softened within the tensile zone.
The outline is shown in Fig.8 and the detailed method which the model established is described below.
a. Horizontal direction
(i) Model of a laminated rubber bearing
The initial stiffness(K1), the second stiffness(K2) and the third stiffness(K3) of the restoring characteristics for the RB were calculated by the static breaking tests of LRBs. Two breaking tests results among the three tests were used, due to the fact that the hysteresis of those tests were similar to each other. The hysteresis of the RB was calculated by removing that of the lead plug from that of the breaking tests of LRB which includes the RB and the lead plug. Then characteristic dissipator shear strength (Qd) of the static tests where the maximum shear strain is 200% was used for the shear force which the lead plug shared. The comparison between the hysteresis of the static breaking tests which shear force were four times as much as the original value and the hysteresis of the polygonal lines is shown in Fig.9. The unloading stiffness was set up using the results of the shaking table tests as the tests for the cyclic loading by where maximum shear strain increases every cycle were

not conducted. The stiffness(K4) used was $20 \times K1$. The stiffness(K5) used the average of the angles which were calculated by approximating the hysteresis under the unloading condition of the shaking table tests at $3 \times S2$ and $4 \times S2$ inputs to the line using the least square method. The repetition influence factor(α) was set up also by using the shaking table tests results. After some of the hysteresis where the maximum shear strain exceeded the previous maximum shear strain in the large loops were chosen, α was calculated by the variation between the value of the strain at the maximum shear force in the loop and that in the previous loop.

(ii) Model of a lead plug

The initial stiffness(Kd) of the lead plug was set up using the static tests results. The hysteresis of the static tests of the LRBs was modeled as a bi-linear model. The second stiffness of the bi-linear model was equal to K1(Fig.8). The initial stiffness of the bi-linear model including K1 was calculated by assuming that the area of the stable loop of the bi-linear model was equal to that of the hysteresis of the static tests. Kd can be calculated by removing K1 from the initial stiffness including K1.

b. Vertical direction

The stiffness(Kc) in the compressive zone used the twice as much as the average of the vertical stiffness of the static tests. The stiffness(Kt) used $1/30 \times Kc$ as its reference[2] as the tests for calculating Kt were not conducted. The yield axial displacement in the tensile zone used the value which was set up based on the static tensile breaking test under non horizontal load and the shaking table tests results.

Analytical Cases

The analyses cases were the same as the shaking table test cases(cf.Table.1).

The Result Of The Simulation Analyses

Time Histories Of The Relative Displacement Of Isolated Layer

The time history of the relative displacement of the isolated layer is shown in Fig.11. The relative displacement – time relation of the simulation analyses was almost the same as the result of the shaking table test at each input level of excitation.

Shear Force – Horizontal Relative Displacement Of Isolated Layer

The relation of the shear force - horizontal relative displacement of the isolated layer is shown in Fig.12. The hysteresis of the simulation analysis at $1 \times S2$ input were within the stable domain (not hardening), which was almost the same as the shaking table test at $1 \times S2$ input. The RB was hardening in the analysis at $2 \times S2$ input as the RB was nearly hardening in the shaking table test.

The histeresis of the analyses at $3 \times S2$ to $5 \times S2$ inputs were almost the same as the shaking table tests in relation to the point of the hardening, the maximum value, the characteristic dissipator shear strength, the initial stiffness(K1) of the RB (cf. Fig.8), etc..

Floor Response Spectra At The Second Floor

Floor response spectra (damping ratio h=1%) at the second floor on which the main equipment was supported are shown in Fig.13. The acceleration value of the floor response spectra for the simulation analysis at $1 \times S2$ input was greater than the shaking table on the whole. That is because the simulation model was set for the amplified S2 inputs in order to confirm the ultimate behavior of the LRB. And although the spectra of the analyses at from $2 \times S2$ to $5 \times S2$ input were a little greater than that of the shaking table tests in the short period domain, these spectra of the analyses were almost the same as that of the shaking table tests over the long period domain which included the base-isolation system's second period(0.5sec).

CONCLUSION

(a) The results of the shaking table tests using the reduced-scaled DFBR model with LRB are summarized as follows.

- The LRB was within the stable domain (not hardening) at $1 \times S2$ input, and were nearly hardening at $2 \times S2$ input. The LRBs did not break at $3 \times S2$ input which was established as the design limit.
- The LRB broke at $5 \times S2$ input, and the failure mode of the bearing which broke first out of the four elements was tension-shear mode.

These results demonstrate that the safety requirement of the LRB was sufficient.

(b) The simulation analyses were conducted for the shaking table tests until the rubber broke. The LRB could be modeled as polygonal lines for a rubber bearing and an elasto-plastic model for a lead plug in the horizontal direction. The results of the analyses are summarized as follows:

- The time histories of the horizontal relative displacement of the isolated layer could simulate the shaking table tests closely at every level input for the hardening point, the maximum value, etc..
- The hysteresis of the shear force – horizontal relative displacement of the isolated layer could also simulate the tests at every level input.
- The floor response spectra on the second floor could almost simulate the tests at every level input.

These results demonstrate that the dynamic behavior of LRB could be simulated closely until the rubber broke by using the polygonal lines.

ACKNOWLEDGEM ENTS

This study was carried out as a part of the FBR common research by the electric power companies in Japan, entitled "Conceptual Design of DFBR". This study was based on the support of Professor T.Fujita of Institute of Industrial Science, University of Tokyo, Japan, which the authors gratefully acknowledged.

REFERENCES

[1] M.KATO, Y.WATANABE, A.KATO, H.KOSHIDA, K.MIZUKOSHI, Y.FUKUSHIMA, O.NOJIMA, G.YONEDA and S.ONIMARU, "*Dynamic Breaking Tests on Base-Isolated FBR Plant*" 12th SMiRT (1993) K22/1

[2] M.KATO, Y.WATANABE, I.HAMA, M.KOYAMA and M.WATANABE, "*Study on Ultimate Behavior of Base Isolated Reactor Building*" 12th SMiRT(1993) K23/5

[3] S.YABANA, Y.OHTORI, K.HIRATA, K.YASUI and T.MAZDA, "*Study on Linear Limits of Rubber Bearings*", AIJ annual report (1996) in Japanese

Table.1 Input condition

TEST NAME	INPUT LEVEL	MAX. ACC. (gal)
DESIGN	1×S2	380
HARDENING	2×S2	760
DESIGN LIMIT	3×S2	1140
BREAKING	4×S2	1520
	5×S2	1900

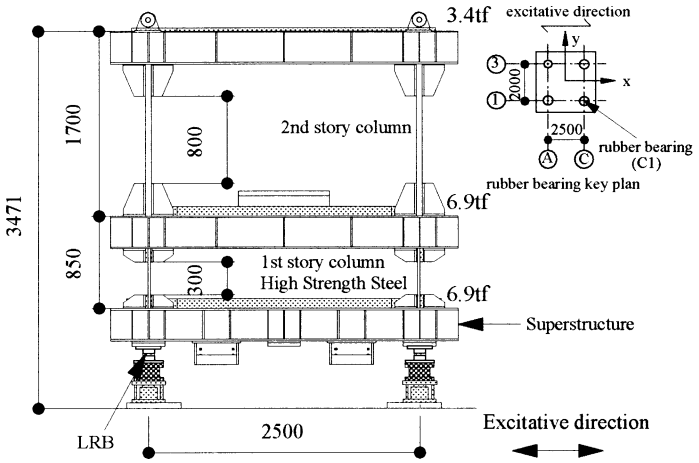

Fig.1 The test model

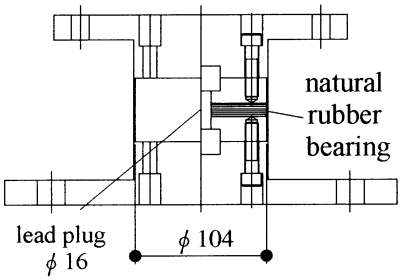

TOTAL THCKNESS OF RUBBER	7mm
A COEFFICIENT OF FIRST FORM	26
A COEFFCIENT OF SECOND FORM	15

Fig.2 The shape of LRB

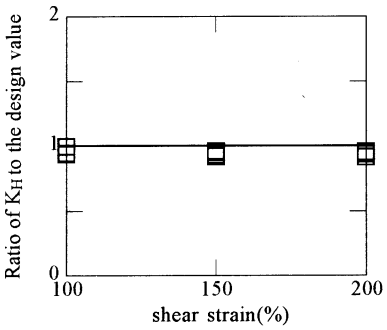

(a) the shear stiffness (KH)

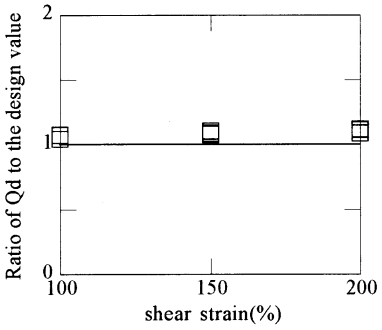

(b) characteristic dissipator shear strength (Qd)

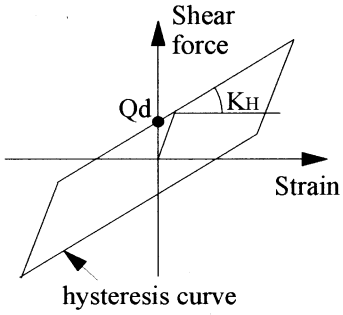

Simplified LRB's hysteresis

Fig. 3 Results of static tests of LRB

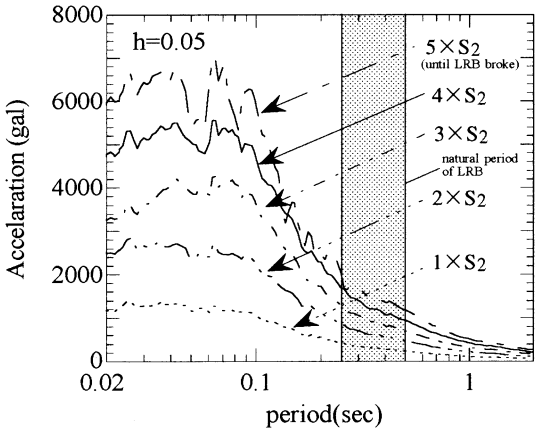

Fig. 4 The acceleration response spectra at the shaking table

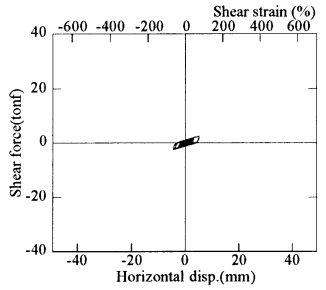

(a) 1×S2 input

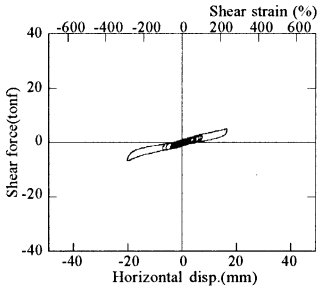

(b) 2×S2 input

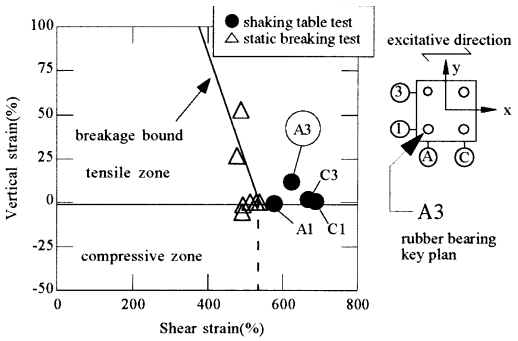

(a) vertical strain-shear strain relation

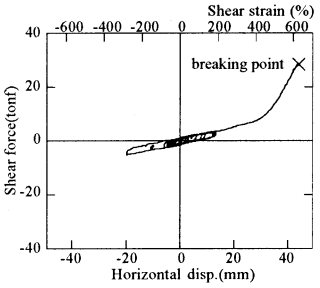

(c) 5×S2 input

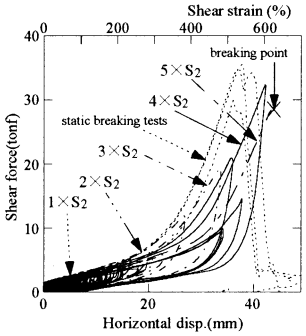

(d) static breakings test and shaking table test

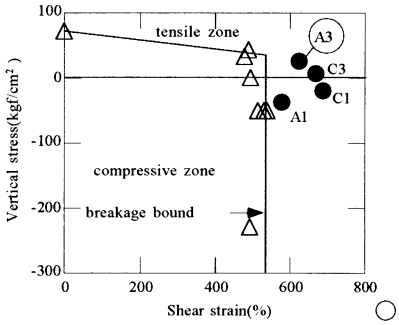

(b) vertical stress-shear strain relation

○: the rubber bearing which broke first

Fig.5 Hysteresis curve of the isolated layer

Fig.6 Failure mode of LRB

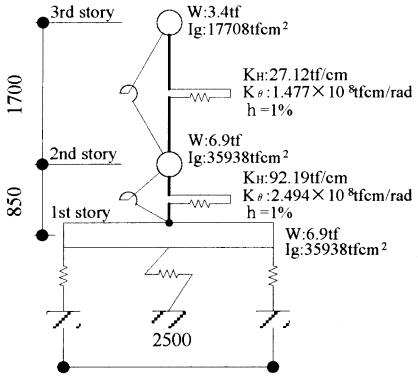

Fig.7 Outline of the simulation model

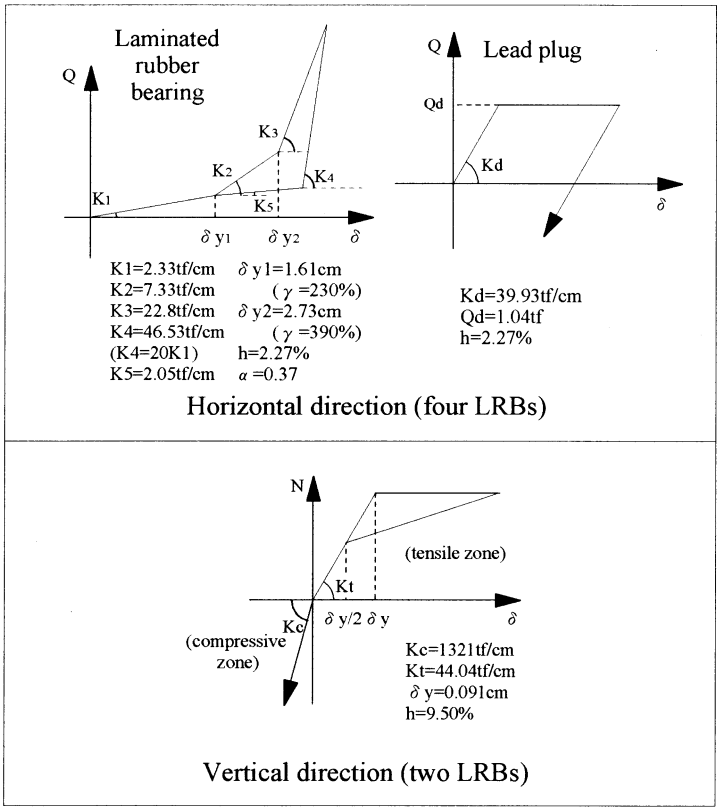

Fig.8 Restoring force characteristics of the isolated layer

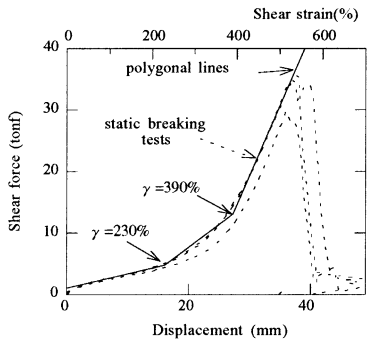

Fig.9 Comparison between static breaking tests and polygonal lines

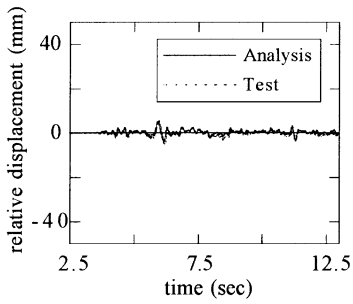

(a) 1×S2

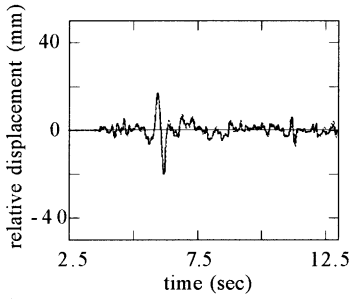

(b) 2×S2

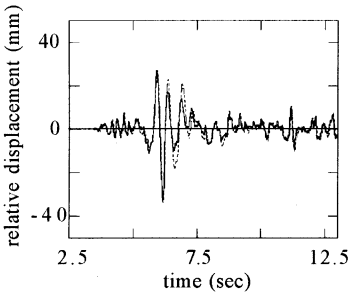

(c) 3×S2

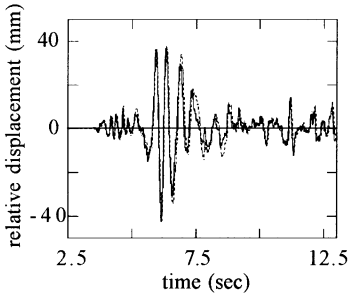

(d) 4×S2

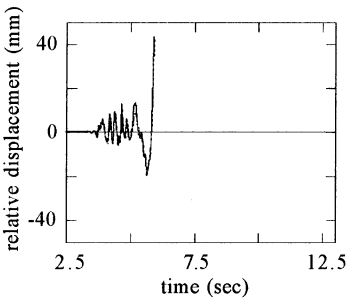

(e) 5×S2

Fig.11 The time histories of horizontal relative displacement at the isolated layer

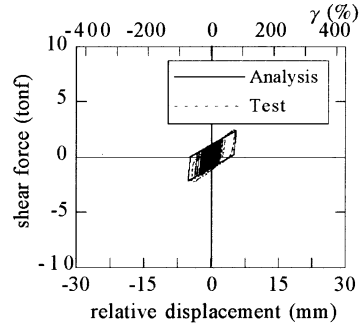

(a) 1×S2

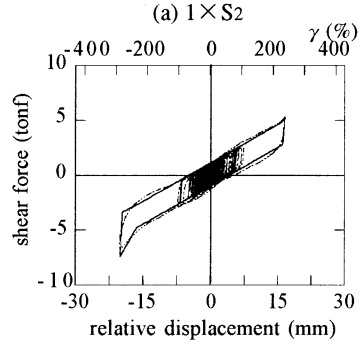

(b) 2×S2

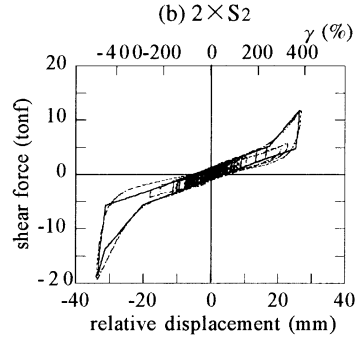

(c) 3×S2

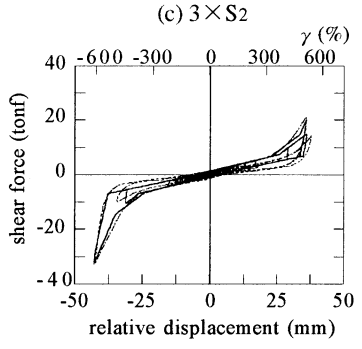

(d) 4×S2

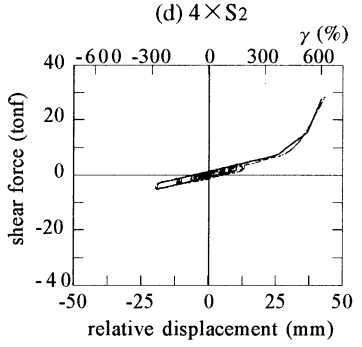

(e) 5×S2

Fig.12 The hysteresis of the isolated layer (shear force-horizontal displacement)

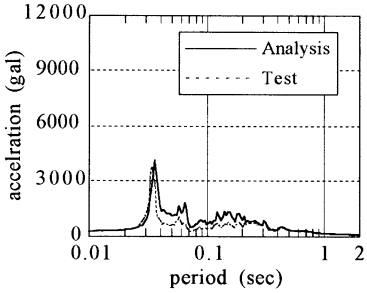

(a) 1×S2

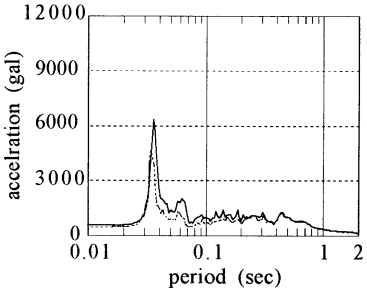

(b) 2×S2

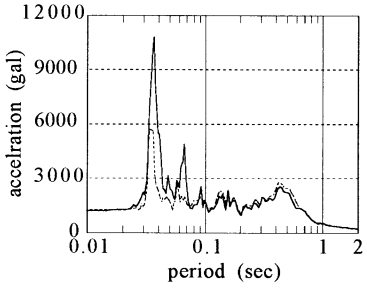

(c) 3×S2

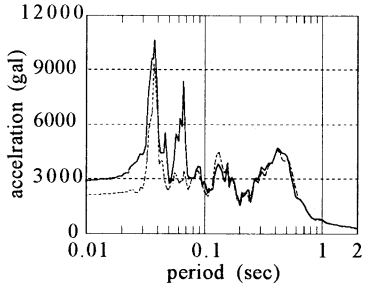

(d) 4×S2

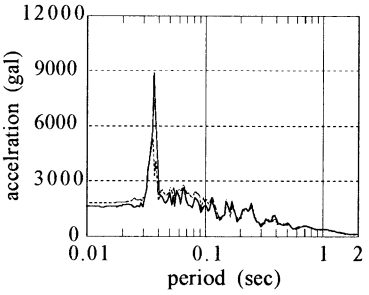

(e) 5×S2

Fig.13 The floor response spectra on the second floor (h=1%)